Current Applied Physics 12 (2012) 663–667

Contents lists available at SciVerse ScienceDirect

Current Applied Physics

journal homepage: www.elsevier.com/locate/cap

One-dimensional solution to the stable, space-charge-limited emission of secondary electrons from plasma-wall interactions

Jongho Seon [a,*], Ensang Lee [a], Wonho Choe [b], Hae June Lee [c]

[a] School of Space Research, Kyung Hee University, 1, Seocheon-dong, Giheung-gu, Yongin-si, Gyeonggi-do, 446-701, Republic of Korea
[b] Department of Physics, Korea Advanced Institute of Science and Technology, 291 Daehak-ro, Daejeon, 305-701, Republic of Korea
[c] School of Electrical and Computer Engineering, Pusan National University, Busan, 609-735, Republic of Korea

ARTICLE INFO

Article history:
Received 25 August 2011
Accepted 6 October 2011
Available online 13 October 2011

Keywords:
Space-charge-limited emission
Secondary electrons
Plasma sheath
Sheath criterion

ABSTRACT

Numerical solutions to the stable, space-charge-limited emission of secondary electrons from plasma-wall interaction are found based on one-dimensional plasma moment equations that assume cold ions, Maxwellian electrons and cold secondary electrons. The numerical method finds a range of plasma parameters that permit stable emission of secondary electrons in the absence of normal electric fields to the wall. These solutions were not obtained with previous method that solves only for the marginally stable plasma sheath. Range of the ion Mach number at the sheath edge, the floating wall potential relative to the plasmas, and secondary electron emission coefficients corresponding to the vanishing normal electric fields are found for hydrogen, argon and xenon plasmas. The results show that a relatively small range of secondary electron emission coefficient exists to allow stable sheaths structures along with larger ranges of ion injection speed at the sheath edge and floating potential of the emitting wall.

1. Introduction

The interaction of plasmas with electrically floating boundary surface generates a charge separation region of plasma sheath where a large electric field exists to balance the electrical currents from the plasmas [1]. It is often possible that the floating boundary can emit significant secondary electrons back to the plasma via various physical mechanisms such as the secondary electron emission, sputtering, thermionic emission or photoionization. The modeling of the plasma sheath in the presence of the secondary electron emission based on steady-state, one-dimensional moment equations of plasmas have been previously made by Hobbs and Wesson [2]. More elaborate and sophisticated modeling of the plasma sheath taking into account the kinetic aspects [3–8], magnetic fields [9–11], and collisions [12–14] has been comprehensively followed. Laboratory examinations of the theories and comparisons have been also made [15–17].

Increasing secondary electron emission from the floating surface generally reduces the magnitude of electric fields because the secondary electron emission decreases the net current toward the wall. As the secondary electron emission further increases, the maximum emission current is attained because at this point the electrons near the surface that were previously emitted, or the space charges, impede further increase of the electron current emission. Therefore, this space-charge-limited regime is considered the maximum plasma interaction of ambient plasmas with the surrounding boundary. Hobbs and Wesson [2] found the solution to this important regime of plasma interaction based on an approximate analytic method for the case of marginally stable sheath. The case is examined by requiring that the obtained electrostatic potential from the Poisson's equation be real at the edge of the plasma sheath. For infinitely massive ions, they found the surface potential of the emitting wall relative to the plasmas, $e\phi_0 \sim -1.02kT$ and ion Mach number M^2 at the sheath edge, $\sim$1.16.

The treatment of Hobbs and Wesson successively solves the plasma continuity equation, the energy equations for ions and Boltzmann relation for electrons, and the Poisson's equation. The marginally stable condition of the plasma sheath is obtained when the first non-vanishing term from the Taylor expansion of the Poisson's equation begins to yield non-imaginary solution. However, additional questions naturally arise as to the existence of the plasma sheath solution beyond the marginal stability because the solution is just obtained at a single point among the allowed range of parametric boundary conditions. As a specific example, if the emission of the secondary electrons becomes stronger, one may ask whether the electric field near the wall change its slope to

* Corresponding author. Tel.: +82 31 201 3282.
E-mail address: jhseon@khu.ac.kr (J. Seon).

1567-1739/$ – see front matter
doi:10.1016/j.cap.2011.10.001

inhibit further emission. Or one may expect that the magnitude of the floating wall potential further lowers itself to support stable, steady-state plasma sheaths by collecting more primary electrons to allow stronger secondary emissions without turning the slope. If the sheath is stable or can be made stable beyond the marginal stability, one may further examine the conditions for the stability of the sheath such as the Bohm's stability condition or the floating wall potential. Finally, but not lastly the nature of new physics, if exists, beyond the regime of the space-charge-limited emission can be investigated.

The purpose of this paper is to answer some of the questions raised above. We will find all the stable solutions from the Hobbs and Wesson equation through numerical method. Especially, Mach number at the plasma sheath, relative potential of the emitting wall, and the secondary electron emission coefficients will be found when the normal electric field vanishes at the wall. This analysis is performed for the case of hydrogen, argon and xenon plasmas.

2. Model equations

In this paper, the basic notion of the plasma presheath and sheath is employed [1,2]. The main body of the plasma is located in the right side of Fig. 1. The left boundary is an infinite planar wall collecting and emitting plasmas. There are three regions, the sheath, presheath and plasma. In the sheath region most of the potential drop between the plasma and the wall exists owing to the charge separation of ions and electrons. The presheath is a region that connects the body of plasmas where somewhat smaller, but not negligible potential drop is expected due to various physical mechanisms such as collisions, inertia and magnetic fields [3–9]. The present study finds solutions valid only in the sheath region. In this section, the equations governing the electric structure in the sheath will be summarized. The equations are basically identical to those used in Hobbs and Wesson [2] in a slight different form for later numerical analysis.

Consider the case of one-dimensional (1-D) plasma sheath for which electron emission from the wall is included. The effect of space charge on the sheath potential near the wall is analyzed by solving the Poisson's equation within the sheath:

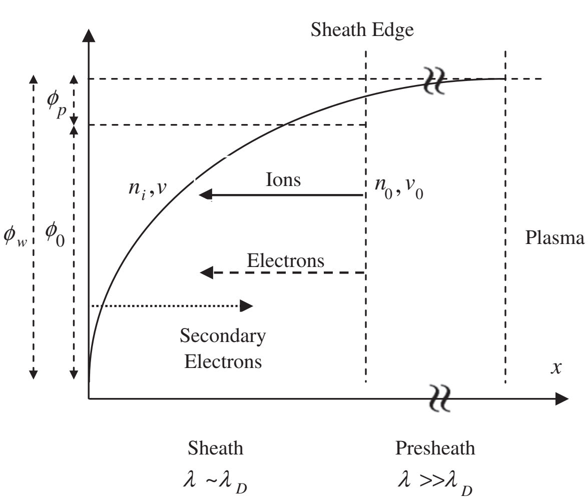

Fig. 1. Concept of presheath and sheath. The potential difference between the plasma and wall is mostly found in the sheath region where charge separation between the plasma species takes places on the order of Debye length scale. The presheath is a region that connects the body of plasmas where somewhat smaller, but not negligible potential drop is expected due to various physical mechanisms such as collisions, inertia and magnetic fields [3–9].

$$\frac{d^2\phi}{dx^2} = \frac{e}{\varepsilon_0}(n_e + n_s - n_i), \tag{1}$$

where n_e, n_s and n_i are the number densities of electrons, secondary electrons and ions, respectively. Assuming a Maxwellian distribution for the electrons, the plasma density in the sheath is:

$$n_e(x) = (n_0 - n_{s0})e^{\frac{e\phi(x)}{k_B T}}. \tag{2}$$

Here n_0 is the ion density at the sheath edge, n_{s0} is the secondary electron density at the sheath edge and ϕ is the potential relative to the asymptotic ambient plasma potential, and k_B and T are Boltzmann's constant and electron thermal temperature, respectively. The ions are assumed cold and arrive at the sheath edge with energy of

$$E = \frac{1}{2} m_i v_0^2. \tag{3}$$

Here v_0 is the ion speed entering the sheath edge, or the Bohm velocity, modified for the presence of secondary electrons. The ion density through the sheath is then determined from the flux and energy conservation to yield:

$$n_i(x) = n_0\sqrt{\frac{E}{E - e\phi(x)}}. \tag{4}$$

The secondary electrons are assumed to be emitted with energy small compared to the plasma electron temperature and are accelerated through the sheath. The equation of continuity for current at the sheath gives, assuming that the secondary electrons are generated by incident electrons, the following relation for the current balance at the wall:

$$I_{ew} = I_{iw} + \gamma I_{ew} \quad \text{or} \quad (1-\gamma)I_{ew} = I_{iw}. \tag{5}$$

Here I_{ew}, I_{iw} and γ and current of primary electrons, ions and secondary electron emission coefficient, respectively. Since the ion current is conserved, it follows that:

$$I_{es} = -en_s v_s = -\frac{e\gamma}{(1-\gamma)} n_0 v_0. \tag{6}$$

The cold secondary electrons are accelerated through the sheath potential. The density of secondary electrons at the sheath is then,

$$n_s = n_0\frac{\gamma}{1-\gamma}\frac{v_0}{v_s} = n_0\frac{\gamma}{1-\gamma}\left(\frac{m_e}{m_i}\frac{E}{e(\phi-\phi_0)}\right)^{\frac{1}{2}}. \tag{7}$$

Here m_e and m_i are the mass of electrons and ions, respectively and ϕ_0 is the value of ϕ at the wall. The value ϕ_0 is usually negative because of large fluxes of incident electrons toward the wall. The Poisson's equation as expressed purely in terms of the potential is obtained by combining equations (2), (4), and (7).

$$\begin{aligned}\frac{d^2\phi}{dx^2} &= \frac{e}{\varepsilon_0}\left((n_0 - n_{s0})e^{\frac{e\phi}{k_B T}} + n_0\frac{\gamma}{1-\gamma}\left(\frac{m_e}{m_i}\frac{E}{e(\phi-\phi_0)}\right)^{\frac{1}{2}} - n_0\sqrt{\frac{E}{E-e\phi}}\right)\\ &= \frac{en_0}{\varepsilon_0}\left(\left(1 - \frac{\gamma}{1-\gamma}\left(-\frac{m_e}{m_i}\frac{E}{e\phi_0}\right)^{\frac{1}{2}}\right)e^{\frac{e\phi}{k_B T}}\right.\\ &\quad\left. + \frac{\gamma}{1-\gamma}\left(\frac{m_e}{m_i}\frac{E}{e(\phi-\phi_0)}\right)^{\frac{1}{2}} - \sqrt{\frac{E}{E-e\phi}}\right).\end{aligned} \tag{8}$$

This second order differential equation can be reduced to the first order by multiplying $d\phi/dx$ on both sides of equation (8) and integrating from the sheath edge to x to get,

$$\frac{\varepsilon_0}{2n_0k_BT}\left(\frac{d\phi}{dx}\right)^2=\left(\left(1-\frac{\gamma}{1-\gamma}\left(-\frac{m_e}{m_i}\frac{E}{e\phi_0}\right)^{\frac{1}{2}}\right)\left(e^{\frac{e\phi}{k_BT}}-1\right)+\frac{2\gamma}{1-\gamma}\sqrt{\frac{m_e}{m_i}\cdot\frac{E}{k_BT}\cdot\frac{-e\phi_0}{k_BT}}\left(\sqrt{1-\frac{\phi}{\phi_0}}-1\right)+\frac{2E}{k_BT}\left(\sqrt{1-\frac{e\phi}{E}}-1\right)\right). \tag{9}$$

The equation is ready to be integrated in principle once the boundary conditions E_0 and ϕ_0 are given. Now introduce the following dimensionless variables:

$$\chi\equiv-\frac{e\phi}{k_BT},\quad \xi\equiv\frac{x}{\lambda_D}=x\sqrt{\frac{n_0e^2}{\varepsilon_0k_BT_e}},\quad \frac{1}{2}M^2=\frac{E}{k_BT}. \tag{10}$$

Then the above equation becomes:

$$\frac{1}{2}\left(\frac{d\chi}{d\xi}\right)^2=\left(M^2\left(\sqrt{1+\frac{2\chi}{M^2}}-1\right)+\left(1-\frac{\gamma}{1-\gamma}\sqrt{\frac{1}{2}\frac{m_e}{m_i}\frac{M^2}{\chi_0}}\right)\left(e^{-\chi}-1\right)+\frac{2\gamma}{1-\gamma}\sqrt{\frac{1}{2}\frac{m_e}{m_i}M^2\chi_0}\left(\sqrt{1-\frac{\chi}{\chi_0}}-1\right)\right). \tag{11}$$

Near the edge of the sheath boundary for which $\chi \ll 1$, usual expansion of the right-hand side of equation (11) to get positive definite yields a relation below for stability of the sheath,

$$M^2\geq\frac{1}{\left(1-\frac{\gamma}{1-\gamma}\sqrt{\frac{1}{2}\frac{m_e}{m_i}\frac{M^2}{\chi_0}}\right)+\frac{1}{2}\left(\frac{\gamma}{1-\gamma}\sqrt{\frac{1}{2}\frac{m_e}{m_i}\frac{M^2}{\chi_0^3}}\right)}. \tag{12}$$

The term on the left-hand side of equation (14) accounts for the current generated by electrons whose density is calculated from the value at the sheath edge with an assumption of Maxwellian velocity distributions. The right-hand side of equation (14) is the ion current term. On the other hand, the space-charge-limited solution is obtained when the electric field of the surface of the emitting wall becomes zero. The zero electric field is obtained when the right-hand side of equation (11) becomes zero:

$$M^2\left(\sqrt{1+\frac{2\chi_0}{M^2}}-1\right)+\left(1-\frac{\gamma}{1-\gamma}\sqrt{\frac{1}{2}\frac{m_e}{m_i}\frac{M^2}{\chi_0}}\right)\left(e^{-\chi_0}-1\right)-\frac{2\gamma}{1-\gamma}\sqrt{\frac{1}{2}\frac{m_e}{m_i}M^2\chi_0}=0. \tag{15}$$

Solving (12), (14) and (15) simultaneously should determine the value of M^2, χ_0 and γ when the electric field normal to the emitting wall vanishes to give a stable, space-charge-limited solution.

3. Numerical method

In order to simultaneously solve equations (12), (14) and (15), the following sequence of analysis is undertaken. There are three unknowns, M^2, χ_0 and γ, to be determined from the equations. Because equation (12) only gives a condition for stable solutions expressed in an inequality form, we solve equations (14) and (15) with respect to M^2 and χ_0 for a given, fixed γ. Then range of γ value will be examined to confirm whether the stability condition (12) is indeed satisfied. If the solution is marginal, the equality of (12) is met. If the solution corresponds to stable sheath, the inequality condition of (12) will be satisfied. This is the solution that the present paper attempts to find. Equations (14) and (15) can be conveniently expressed in the following form:

$$\mathbf{F}=\begin{pmatrix}F_1\\F_2\end{pmatrix}\equiv\begin{pmatrix}\left((1-\gamma)-\gamma\left(\frac{m_e}{2m_i}\frac{M^2}{\chi_0}\right)^{\frac{1}{2}}\right)e^{-\chi_0}-\sqrt{2\pi\frac{m_e}{m_i}M^2}\\ M^2\left(\sqrt{1+\frac{2\chi_0}{M^2}}-1\right)+\left(1-\frac{\gamma}{1-\gamma}\sqrt{\frac{1}{2}\frac{m_e}{m_i}\frac{M^2}{\chi_0}}\right)\left(e^{-\chi_0}-1\right)-\frac{2\gamma}{1-\gamma}\sqrt{\frac{1}{2}\frac{m_e}{m_i}M^2\chi_0}\end{pmatrix}=0. \tag{16}$$

Another important boundary condition is found by requiring that the total current be zero at the wall. Now the electron density at the sheath edge is related to the density of ion and secondary electrons by the relation (7):

$$n_{e0}=n_0-n_{s0}=n_0\left(1-\frac{\gamma}{1-\gamma}\left(-\frac{m_e}{m_i}\frac{E}{e\phi_0}\right)^{\frac{1}{2}}\right). \tag{13}$$

The current balance relation $(1-\gamma)I_{ew}=I_{iw}$ that has to be met by the incoming ions and electrons and emitted secondary electrons at the wall gives a relation below:

$$\left((1-\gamma)-\gamma\left(\frac{m_e}{2m_i}\frac{M^2}{\chi_0}\right)^{\frac{1}{2}}\right)e^{-\chi_0}=\sqrt{2\pi\frac{m_e}{m_i}M^2}. \tag{14}$$

The solution to this equation can be obtained with the Newton–Raphson method [18] which iteratively solves the following equations:

$$\mathbf{J}\cdot\delta\mathbf{x}=-\mathbf{F}, \tag{17}$$

and,

$$\mathbf{x}_{new}=\mathbf{x}_{old}+\delta\mathbf{x}, \tag{18}$$

where,

$$\mathbf{x}=\begin{pmatrix}x_1\\x_2\end{pmatrix}=\begin{pmatrix}M^2\\\chi_0\end{pmatrix}. \tag{19}$$

Here the Jacobian is defined as follows:

$$\mathbf{J}=\frac{\partial(F_1,F_2)}{\partial(x_1,x_2)}. \tag{20}$$

The Newton–Raphson method can be easily applied to this problem because the Jacobian, equation (20), is analytically determined from equation (16). The Newton–Raphson method requires an initial guess of a solution and different solutions, if exist, can be obtained by different initial guesses. For the initial guess large range of M^2 and χ_0 values of is swept. If there is a converging solution, the iteration stops and accepts values for subsequent analysis. The criterion for the convergence is to have absolute magnitude of each F_1 and F_2 less than 10^{-8}.

The sign of **F** in equation (16) at neighboring points around the obtained solutions is estimated to examine if **F** changes sign to yield zeroes of the equations. If the solution passes the aforementioned criteria, equation (12) is finally examined to determine stability of the sheath. If the stability condition is satisfied, the assumed γ along with the obtained M^2 and χ_0 are accepted as a set of solutions to the equations. The procedure is repeated for a range of γ values from $\gamma = 0$ for which no emission is allowed to $\gamma = 1$ above which no more solution from the steady-state equations evidently exists. The latter can be easily confirmed with an inspection of equation (16) because all the terms in F_1 become negative above $\gamma = 1$. Therefore, no more solution can be found above $\gamma = 1$.

4. Results and discussions

Fig. 2 summarizes the results of the numerical methods described in the previous section. The two graphs in the figures correspond to the solutions for the Mach number M^2 and the floating potential of the wall χ_0 determined from equations (14) and (15). The horizontal axis represents the secondary electron emission coefficients γ in obtaining the solutions. As the emission coefficient γ varies from 0 to 1, it is found that there exists three occasions: 1) the solution does not meet stability criterion, 2) the solution meets the criterion, and 3) no solution is found. The boundary of each region of γ separating these occasions is designated with vertically dashed lines at γ_1 and γ_2, in the figure. Below γ_1 the stability condition is not satisfied, whereas no physical solution is found above γ_2. The solutions that we look for are found between γ_1 and γ_2 and plotted in red. The marginally stable case corresponds to the solution at γ_1. This case was previously examined with an analytic method by Hobbs and Wesson [2] (For interpretation of the references to color in this paragraph, the reader is referred to the web version of this article.).

The existence of the numerical solution is demonstrated in Fig. 3 by showing that each function of the equation actually changes sign as a function of χ_0 and M^2 for properly assumed values of γ. The top panels show variation of F_1 and F_2 corresponding to the emission coefficient γ_1. For (a), M^2 value is fixed, whereas variation of F_1 and F_2 are shown as a function of χ_0. For (b), F_1 and F_2 are shown as a function of M^2. The fixed values are the solutions obtained from the analysis. Similarly, the variations of F_1 and F_2 corresponding to the emission coefficient γ_2 are shown in (c) and (d) as functions of χ_0 and M^2. All the plots show that the functions change sign across the solutions from the numerical analysis. These plots are for xenon plasmas. The existence of the solution is also verified for hydrogen and argon plasmas.

The numerical results from the previous section show that there is a range of parameters that correspond to the stable plasma sheath with zero electric fields at the emitting wall. For example, for the case of hydrogen plasma, marginally stable secondary electron emission is found near $\gamma \sim 0.82$, $M^2 \sim 1.04$, $\chi \sim 1.01$ as indicated in Fig. 2. This is comparable to the result by Hobbs and Wesson for space-charge-limited emission near $\gamma \sim 0.81$, $M^2 \sim 1.16$, $\chi_0 \sim 1.02$. The calculated numbers reasonably agree well for γ and χ_0, but significant improvement of the numerical accuracy is made for M^2. The present result further shows that there exists a range of

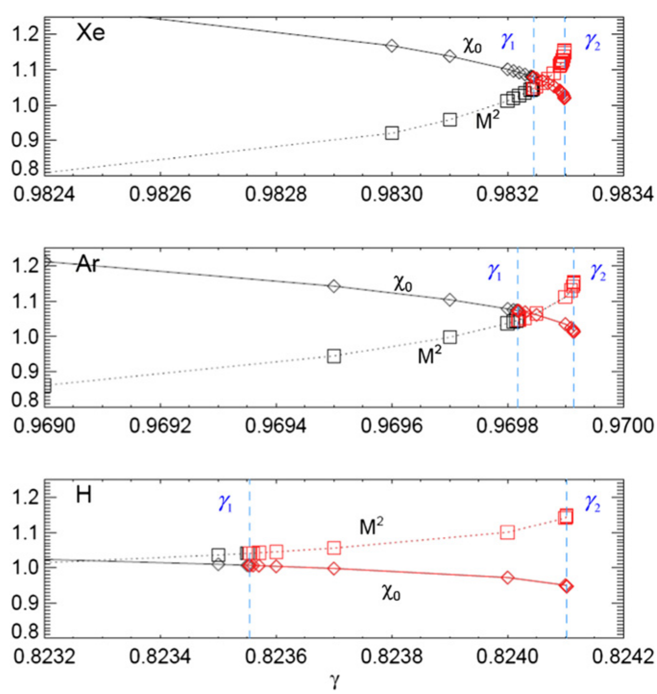

Fig. 2. Numerical solution to the stable, space-charge-limited emission. The solution is found by first simultaneously solving equations (14) and (15) for a given γ. The stability condition (12) is then examined to determine whether the obtained solution corresponds to the stable sheath. If the stability condition is satisfied, it is plotted in red. The solution is found between the two vertically dashed lines at γ_1 and γ_2 in the figure. The marginally stable solution corresponds to the left vertically dashed line γ_1. Below γ_1, the stability condition is not met, whereas above γ_2 no physical solution exists. (For interpretation of the references to color in this figure legend, the reader is referred to the web version of this article.).

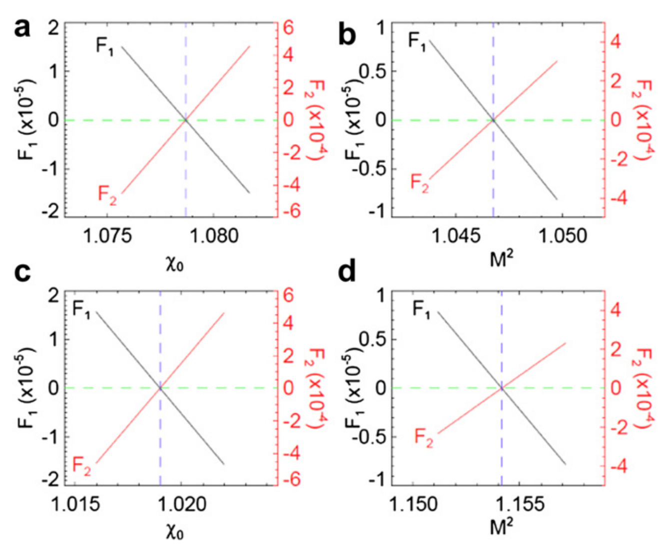

Fig. 3. Existence of the solution to equation (16). The existence of the solution to the equation is demonstrated by showing that, for assumed value of γ, each function of the equation actually changes sign as one of χ_0 and M^2 is varied, whereas the other remains fixed. The top panels show variation of F_1 and F_2 corresponding to the emission coefficient γ_1. For (a), M^2 value is fixed to show variations of F_1 and F_2 as a function of χ_0, while F_1 and F_2 are shown as a function of M^2 in plot (b). The fixed values are the solutions obtained from the analysis. Similarly, the variations of F_1 and F_2 corresponding to the emission coefficient γ_2 are shown in (c) and (d) as functions of χ_0 and M^2. These plots are for xenon plasmas. The existence of the solution is also verified for hydrogen and argon plasmas.

Table 1
Numerical solutions to the equations for stable, space-charge-limited emission of secondary electrons for xenon, argon and hydrogen plasmas. The numbers in the table are secondary electron emission coefficient γ, square of the Mach number evaluated at the sheath edges ($M^2 = m_i v_0^2/k_B T$), and relative potential of the wall ($\chi_0 = -e\phi_0/k_B T$), respectively. There is a range of these parameters identified from the analysis consistent with stable plasma sheath with zero electric field at the emitting wall. Maximum and minimum values are shown for xenon, argon and hydrogen plasmas.

	γ	M^2	χ_0
Xe	0.98324	1.05	1.08
	0.98329	1.15	1.02
Ar	0.96981	1.05	1.07
	0.96991	1.15	1.01
H	0.82355	1.04	1.00
	0.82410	1.15	0.95

plasma parameters that allow secondary electron emissions with vanishing electric fields. Note that the allowed range of γ from the calculation is relatively small. However, the corresponding variation of the sheath Mach number M^2 and the floating potential of the wall χ_0 are substantial. Similar results for argon and xenon plasmas are shown in the figure and are summarized in Table 1.

In the introduction, a question has been raised whether the magnitude of the floating wall potential can further decrease to allow stronger secondary emissions beyond the marginal stability. Our calculation suggests a positive answer to this question. This should be compared to the common expectation that the slope of electric field should change its sign to inhibit further emission of electrons beyond the marginal stability of the space-charge-limited sheath. It turned out that the stability of space-charged-limited emission is possible for a narrow range of secondary electron emission coefficient (γ), but for a relatively large range of ion speed at the sheath edge (M^2) and the floating wall potential (χ_0). Investigation of the obtained solutions show that stable space-charge-limited emission is possible by lowering the floating potential, while requiring higher ion speed at the sheath edge for more ion current injection. This relative trend of χ_0 and M^2 is clearly explained in Fig. 3. In this case of stronger emission, the current balance as required for a steady-state solution is maintained by 1) increased primary electron current to the wall due to lower magnitude of the floating wall potential, 2) increased secondary electron current due to stronger emission, 3) and increased ion current due to stronger injection at the sheath edge. However, the present study further shows that this stable secondary emission is possible only for a limited range of (γ, M^2, χ_0). The condition for the stability is 1.04–1.15 for M^2 and 0.95–1.00 for χ_0. They are not negligible. We also calculated the stability criterion for other ion species such as Ar and Xe. The comparison shows that the range of M^2 remains relatively the same, but floating potential changes significantly for different ion species.

It should be noted that the present analysis only finds a sheath solution with vanishing electric fields at the wall because we first request that equation (8), the integrated Poisson equation evaluated at the wall, be zero together with current balance equation. For any solution found at smaller values of γ_1, it only means that this numerical analysis finds it inconsistent to simultaneously meet the conditions of sheath stability and zero electric fields at the wall. The possibility of having stable sheath with non-vanishing electric fields at the wall validly exists and is not addressed by the current method.

On the other hand, above γ_2, it turns out that that the current balance equation (14) does not hold because the left-hand side can change sign as the secondary electron emission coefficient γ increases. The right-hand side, on the other hands, must be always positive definite. The sign change of the left-hand side of equation (14) from positive to negative value occurs at γ_2. Therefore, there is no steady-state solution above γ_2. This is due to the violation of the current balance at the wall and violation of quasi-charge neutrality at the sheath edge. If a steady-state solution is forbidden, it is plausible to expect oscillatory behavior of the sheath. Recent numerical simulation has found oscillatory behavior of plasma sheath when the secondary electron emission coefficient becomes larger than a critical value in plasma devices [19–21]. Such behaviors of the plasma sheath are not adequately described with the present analysis that assumes steady-state of the plasmas and may be described with time-dependent form of the equations.

Acknowledgement

This research was supported by National Space Lab (NSL) (Grant No.: 2009-0091569) and World Class University (WCU) (Grant No.: R31-10016) programs through the National Research Foundation of Korea funded by the Ministry of Education, Science and Technology.

References

[1] D. Bohm, in: A. Guthrie, R. Wakering (Eds.), The Characteristics of Electrical Discharges in Magnetic Fields, McGraw-Hill, New York, 1949.
[2] Hobbs, Wesson, Heat flow through a Langmuir sheath in the presence of electron emission, Plasma Phys. 9 (1967) 85–87.
[3] G.A. Emmert, R.M. Wieland, A.T. Mense, J.N. Davidson, Electric sheath and presheath in a collisionless, finite ion temperature plasma, Phys. Fluids 23 (1980) 803–812.
[4] R.J. Procassini, C.K. Birdsall, E.C. Morse, A fully kinetic, self-consistent particle simulation model of the collisionless plasma–sheath region, Phys. Fluids (B) 2 (1990) 3192–3205.
[5] K.-U. Riemann, The Bohm criterion and sheath formation, J. Phys. D: Appl. Phys. 24 (1991) 493–518.
[6] L.A. Schwager, Effects of secondary and thermionic electron emission on the collector and source sheaths of a finite ion temperature plasma using kinetic theory and numerical simulation, Phys. Fluids (B) 5 (2) (1993) 631–646.
[7] K.F. Stephens II, C.A. Ordonez, Sheath and presheath potentials for anode, cathode and floating plasma-facing surfaces, J. Appl. Phys. 85 (5) (1999) 2522–2528.
[8] L. Jolivet, J. Roussel, Numerical modeling of plasma sheath phenomena in the presence of secondary electron emission, IEEE Trans. Plasma Sci. 30 (2002) 318–326.
[9] R. Chodura, Plasma–wall transition in an oblique magnetic field, Phys. Fluids 25 (1982) 1628–1634.
[10] E. Ahedo, Structure of the plasma-wall interaction in an oblique magnetic field, Phys. Plasmas 4 (12) (1997) 4419–4430.
[11] I.I. Bellis, M. Keidar, Sheath and presheath structure in the plasma-wall transition layer in an oblique magnetic field, Phys. Plasmas 5 (5) (1998) 1545–1553.
[12] K.-U. Riemann, The influence of collisions on the plasma sheath transition, Phys. Plasmas 4 (1997) 4158–4167.
[13] X.P. Chen, Sheath criterion and boundary conditions for an electrostatic sheath, Phys. Plasmas 5 (3) (1998) 804–808.
[14] S. Wang, A.E. Wendt, Sheath thickness evaluation for collisionless or weakly collisional bounded plasmas, IEEE Trans. Plasma Sci. 27 (5) (1999) 1358–1365.
[15] L. Oksuz, N. Hershkowitz, First experimental measurements of the plasma potential throughout the presheath and sheath at a boundary in a weakly collisional plasma, Phys. Rev. Lett. 89 (2002) 145001–145004.
[16] N. Hershkowitz, Sheaths: more complicated than you think, Phys. Plasmas 12 (5) (2005) 055502–055513.
[17] G.D. Severn, X. Wang, E. Ko, N. Hershkowitz, Experimental studies of the Bohm criterion in a two-ion-species plasma using laser-induced fluorescence, Phys. Rev. Lett. 90 (14) (2003) 145001–145005.
[18] W.H. Press, S.A. Teukolsky, W.T. Vetterling, B.P. Flannery, Numerical Recipes in C, The Art of Scientific Computing, second ed. Cambridge University Press, Cambridge, 1992, p. 362.
[19] D. Sydorenko, A. Smolyakov, I. Kaganovich, Y. Raitses, Plasma-sheath instability in Hall thrusters due to periodic modulation of the energy of secondary electrons in cyclotron motion, Phys. Plasmas 15 (5) (2008) 053506–053513.
[20] D. Sydorenko, I. Kaganovich, Y. Raitses, A. Smolyakov, Breakdown of a space charge limited regime of a sheath in a weakly collisional plasma bounded by walls with secondary electron emission, Phys. Rev. Lett. 103 (14) (2009) 145004–145008.
[21] F. Zhang, D. Yu, Y. Ding, H. Li, The spatiotemporal oscillation characteristics of the dielectric wall sheath in stationary plasma thrusters, Appl. Phys. Lett. 98 (2011) 111501–111504.